Theoretical Study of the Benzyl + O_2 Reaction: Kinetics, Mechanism, and Product Branching Ratios

Yoshinori Murakami,*,† Tatsuo Oguchi,‡ Kohtaro Hashimoto,§ and Yoshio Nosaka†

Department of Chemistry, Nagaoka University of Technology, Kamitomioka, Nagaoka, 940-2188, Japan, Department of Ecological Engineering, Toyohashi University of Technology, Toyohashi, 441-8580, Japan, and Honda R&D Co. Ltd. Fundamental Technology Research Center, 1-4-1 Chuo, Wako-shi, Saitama, 351-0193, Japan

Received: July 10, 2007; In Final Form: October 3, 2007

Ab initio calculations at the level of CBS-QB3 theory have been performed to investigate the potential energy surface for the reaction of benzyl radical with molecular oxygen. The reaction is shown to proceed with an exothermic barrierless addition of O_2 to the benzyl radical to form benzylperoxy radical (**2**). The benzylperoxy radical was found to have three dissociation channels, giving benzaldehyde (**4**) and OH radical through the four-centered transition states (channel B), giving benzyl hydroperoxide (**5**) through the six-centered transition states (channel C), and giving O_2-adduct (**8**) through the four-centered transition states (channel D), in addition to the backward reaction forming benzyl radical and O_2 (channel E). The master equation analysis suggested that the rate constant for the backward reaction (E) of $C_6H_5CH_2OO \rightarrow C_6H_5CH_2 + O_2$ was several orders of magnitude higher that those for the product dissociation channels (B−D) for temperatures 300−1500 K and pressures 0.1−10 atm; therefore, it was also suggested that the dissociation of benzylperoxy radicals proceeded with the partial equilibrium between the benzyl + O_2 and benzylperoxy radicals. The rate constants for product channels B−D were also calculated, and it was found that the rate constant for each dissociation reaction pathway was higher in the order of channel D > channel C > channel B for all temperature and pressure ranges. The rate constants for the reaction of benzyl + O_2 were computed from the equilibrium constant and from the predicted rate constant for the backward reaction (E). Finally, the product branching ratios forming CH_2O molecules and OH radicals formed by the reaction of benzyl + O_2 were also calculated using the stationary state approximation for each reaction intermediate.

1. Introduction

The benzyl radical ($C_6H_5CH_2$) plays an important role in the oxidation and pyrolysis of toluene ($C_6H_5CH_3$) and alkyl-substituted benzene molecules. However, since the benzyl radical is an unusual radical in that it is conjugatively stabilized and does not possess any carbon−carbon bonds that undergo facile scission reactions, the benzyl radicals were regarded as the long-lived species and not capable of initiating chain reactions, even at high temperatures.[1] On the other hand, it has been reported by Brezinsky et al.[2] that a large amount of benzaldehyde (C_6H_5CHO) was formed during the oxidation of toluene in a turbulent adiabatic flow reactor at temperatures around 1000 K under atmospheric pressure. Barnard et al.[3] also found that benzaldehyde was one of the major products in the low-temperature oxidation of toluene between 723 and 788 K. The plausible mechanism for benzaldehyde formation by the low-temperature oxidation of toluene is now considered as follows

$$C_6H_5CH_2 + O \rightarrow C_6H_5CHO + H \quad (1)$$

and

$$C_6H_5CH_2 + HO_2 \rightarrow C_6H_5CH_2O + OH \quad (2a)$$

$$C_6H_5CH_2O \rightarrow C_6H_5CHO + H \quad (2b)$$

Besides the radical−radical reactions responsible for the formation of benzaldehyde shown above, Clothier et al.[4] calculated the reaction pathway forming benzaldehyde using semiempirical MNDO quantum chemical calculations and concluded that benzaldehyde could be formed directly by the reaction of benzyl radical with molecular oxygen through the four-centered intermolecular isomerization reaction

$$C_6H_5CH_2 + O_2 \rightarrow C_6H_5CHO + OH \quad (3)$$

However, further detailed theoretical investigations on the potential energy surface for the reaction of benzyl radical with molecular oxygen have not been carried out so far.

Compared to the numerous experimental[5,6] and theoretical[7,8] studies on the kinetics for the decomposition of benzyl radicals, relatively fewer experiments were performed on the kinetic for the reaction of benzyl + O_2. Since the reactions of hydrocarbon radicals (R) with molecular oxygen are directly linked to the combustion phenomena such as cool flames, engine knock, ignition, and induction times,[9] extensive efforts have been paid for evaluating the rate constants and the equilibrium constants for the reaction of R + O_2.[10,11] The rate constant for the benzyl

* To whom correspondence should be addressed. E-mail: murakami@chem.nagaokaut.ac.jp.
† Nagaoka University of Technology.
‡ Toyohashi University of Technology.
§ Honda R&D Co. Ltd.

10.1021/jp075369q CCC: $37.00
Published on Web 11/28/2007

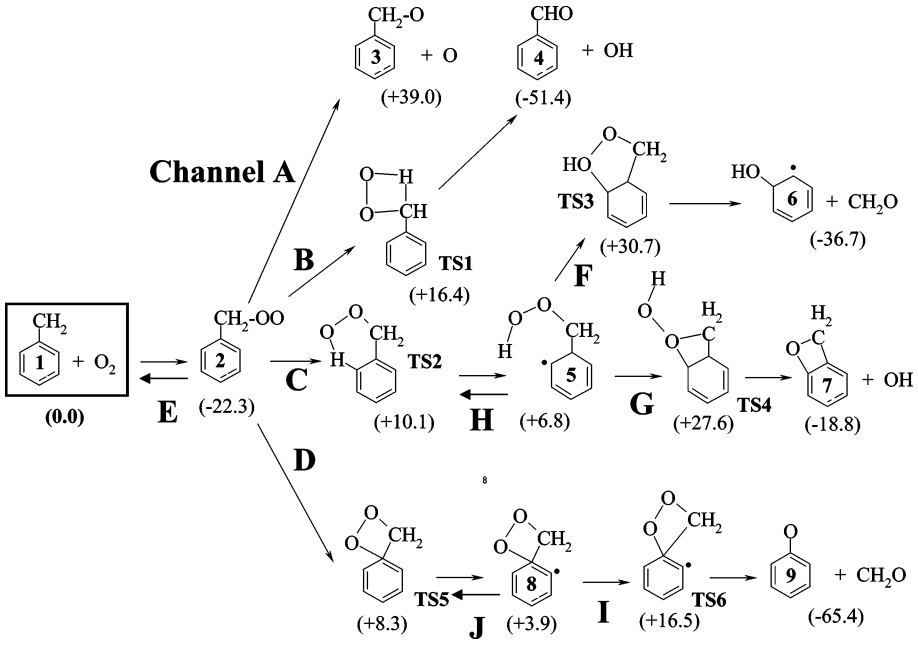

Figure 1. Possible reaction pathways for the benzyl + O_2 reaction. Relative energies of the reactants, products, intermediates, and the transition states are given in kcal/mol as calculated at the CBS-QB3 (in parentheses) level of theory.

+ O_2 reaction has also already been measured by laser flash photolysis[12−14] and discharge flow techniques,[15,16] and the equilibrium constant between benzyl + O_2 and benzylperoxy radicals was also evaluated.[14,16] However, the reaction mechanism for the reaction of benzyl + O_2 above 500 K, which is important for modeling the combustion of toluene and the other alkylbenzenes in motored engines, etc., have not been fully understood.

In the present work, ab initio quantum chemical calculations for the benzyl + O_2 reaction were performed to develop the reaction kinetics for benzyl + O_2 at high temperatures above 500 K. The geometries and the barrier heights for the isomerization reactions of the benzyl peroxide including the four-centered intermolecular isomerization reaction proposed by Clothier et al.[4] were also calculated and not only the overall rate constant for the reaction of benzyl + O_2 but also the plausible dissociation channels for the benzylperoxy radicals, which might be important for understanding the modeling and the product distributions of the toluene combustion, were investigated.

2. Calculation Methods

All quantum chemical computations have been performed with the Gaussian 03 programs.[17] The geometries of the reactants, products, various intermediates, and transition states for the benzyl + O_2 reaction were examined using the density functional theory (DFT) at the B3LYP/6-311G(2d,p,p) level of theory, followed by analytical frequency calculations at the same level to verify that the stationary points were properly located (one imaginary frequency for a transition state and all positive frequencies for a minimum) and also to determine the zero point energies (ZPE) for the stationary points. The intrinsic reaction coordinate (IRC) procedure was used to follow the reaction path from the transition state to reactants and products. Energies at the stationary points were further refined using the procedures of the complete basis method CBS-QB3 developed by Petersson and co-workers.[18,19] The CBS-QB3 is a multilevel model chemistry that combines the results of several electronic structure calculations and empirical terms to predict molecular energies with high accuracy and relatively low computational costs. The required electronic structure calculations are outlined as follows: (i) B3LYP/6-311G(2d,d,p) geometry optimization and frequencies, (ii) MP2/6-311G(3df,2df,2p) energy and CBS extrapolation, (iii) MP4(SDQ)/6-31G(d(f),p) energy, and (iv) CCSD(T)/6-31+G(d′) energy. According to the previous investigations,[19] the CBS-QB3 gives gas-phase energies with an average error of approximately 1 kcal mol^{-1} as compared with experimentally measured values for the G3 set.[20]

Rice−Ramsperger−Kassel−Marcus/Master Equation (RRKM/ME) calculations were carried out using the UNIMOL program of Gilbert and Smith[21] to obtain thermal rate constants for the multichannel dissociation reactions of benzylperoxy radicals. The microcanonical rate constant, $k(E)$, was calculated from the standard form

$$k(E) = W(E-E_0)/h\rho(E) \quad (4)$$

where $W(E)$ denotes the sum of states of the transition state, E_0 is the corresponding threshold energy, h is Planck's constant, and $\rho(E)$ is the density of states for benzylperoxy radicals. In the present RRKM/ME calculations, the conservation of angular momentum was included only in the case of the high-pressure limit. The Lennard-Jones parameters for the benzylperoxy radicals were estimated to be $\sigma = 5.62$ Å and $\epsilon = 617$ K using the method suggested by Gilbert and Smith,[22] and the Lennard-Jones parameters for N_2 as the collision pairs of the benzylperoxy radicals were taken from a reference book.[23] The probability density function for collision energy transfer used was the single exponential-down model:

$$P(E,E') = N(E')^{-1} \exp(-(E' - E)/\langle\Delta E_{down}\rangle) \quad \text{for } E < E' \quad (5)$$

where $N(E')$ is a normalization factor and $\langle\Delta E_{down}\rangle$ is the parameter that is equal to an average energy transferred per collision in the single exponential down model.

3. Results and Discussions

3.1. Potential Energy Surfaces and Reaction Mechanism. Clothier et al.[4] have already calculated reaction channel B

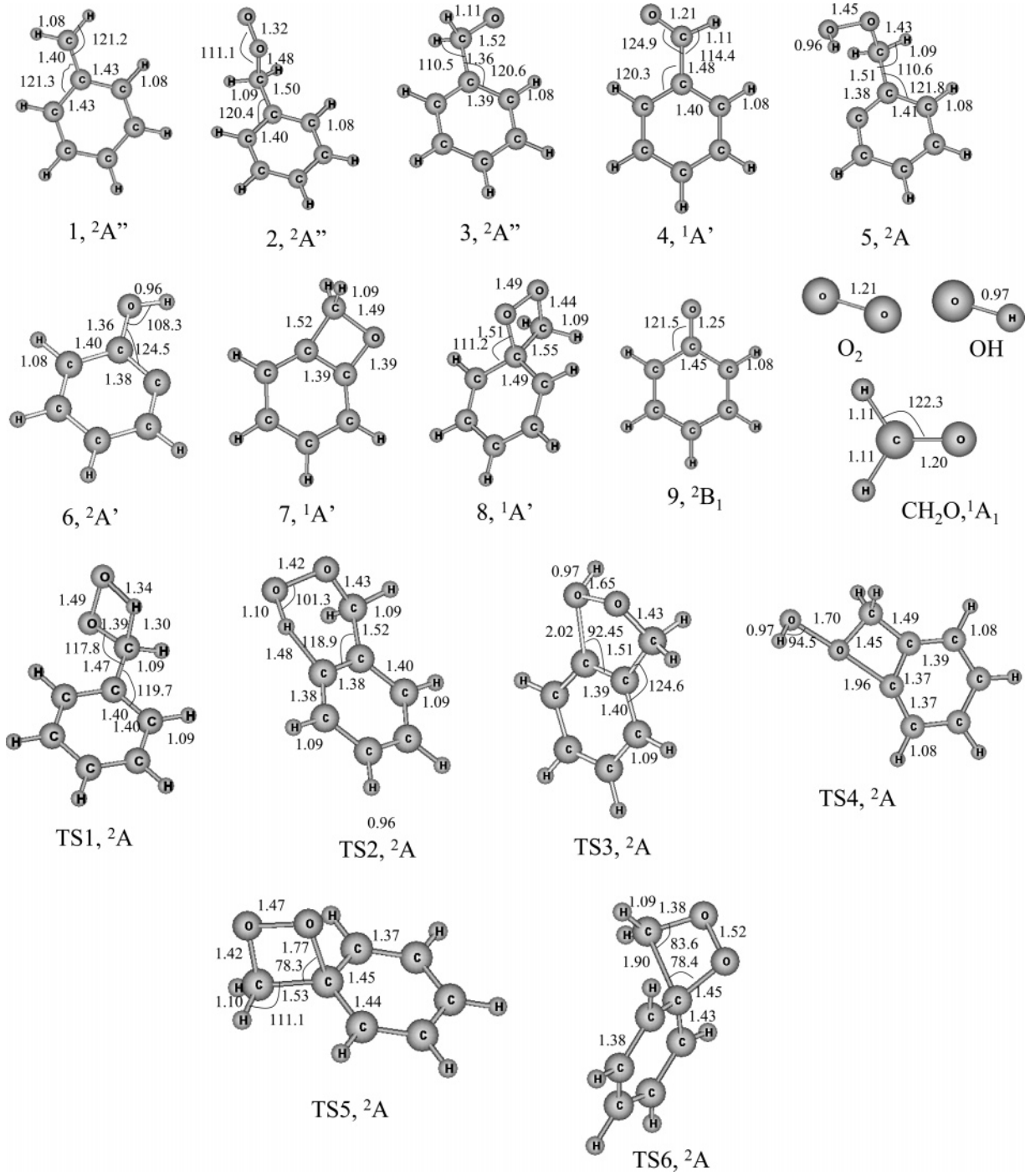

Figure 2. Optimized geometrical parameters of the reactants, the products, the intermediates, and the transition states at the B3LYP/6-311G-(2d,d,p) level of theory. Bond lengths and angles are in Å and deg, respectively.

forming benzaldehyde (**4**) and OH radical through the four-centered intermolecular isomerization reactions of benzyl peroxide (**2**) with semiempirical quantum chemical calculations. In the present work, we calculated the same reaction channel at a higher level of theory; furthermore, we also calculated the other isomerization reaction channels of benzyl peroxide (C_6H_5-CH_2OO, **2**) formed by the addition of molecular oxygen to the benzyl radicals. The first is reaction channel C, which abstracts H atoms at the benzene ring through the six-centered transition state. The second is reaction channel D, which forms O_2-adduct on the benzene ring, followed by the dissociation reaction to form phenoxy (C_6H_5O, **9**) and formaldehyde (CH_2O). The direct abstraction channel (A) forming O atom and $C_6H_5CH_2O$ radical (**3**), which might play the key roles at relatively higher temperature, was also calculated. The schematic figures for the benzyl + O_2 reaction channels considered in the present study are illustrated in Figure 1. Optimized geometric structures for the reactants, the products, and the transition states calculated at the B3LYP/6-311G(2d,d, p) level of theory are also shown in Figure 2. Table 1 lists the rotational constants and the unscaled vibrational frequencies for the reactants, the products, and the transition states used for the kinetic evaluations. To obtain more accurate energies, the CBS-QB3 calculations optimized at the B3LYP/6-311G(2d,d,p) level of theory were carried out. Table 2 summarizes the relative energies with B3LYP/6-311G(2d,d,p), CCSD(T)/6-31G+(d'), MP4(SDQ)/6-31G(d(f),p), and CBS-QB3 levels of theory, respectively. The relative energies at the CBS-QB3 level of theory tabulated in

TABLE 1: Rotational Constants and Vibrational Frequencies of the Intermediates and Transition States in the Benzyl + O_2 System

species	rotational constant (GHz)	frequencies (cm^{-1})
$C_6H_5CH_2$	5.55, 2.71, 1.82	198, 359, 390, 478, 502, 534, 628, 684, 707, 774, 829, 831, 898, 970, 971, 989, 995, 1036, 1117, 1175, 1185, 1288, 1329, 1352, 1474, 1490, 1503, 1 578, 1599, 3145, 3159, 3161, 3173, 3178, 3191, 3241
O_2	43.5	1641
2	4.56, 0.91, 0.81	30, 69, 107, 293, 334, 382, 414, 512, 618, 636, 713, 764, 839, 856, 905, 95 5, 958, 981, 1010, 1020, 1051, 1110, 1177, 1185, 1204, 1212, 1237, 1341, 1360, 1376, 1487, 1493, 1532, 1630, 1650, 3068, 3125, 3162, 3165, 3174, 3183, 3193
3	5.05, 1.51, 1.17	35, 185, 216, 406, 423, 428, 535, 613, 634, 714, 760, 802, 862, 928, 985, 1009, 1017, 1047, 1071, 1104, 1032, 1181, 1191, 1208, 1306, 1332, 1348, 1369, 1484, 1527, 1629, 1646, 2864, 2865, 3145, 3163, 3174, 3186, 3195
4	5.25, 1.56, 1.21	123, 221, 242, 419, 443, 469, 631, 663, 708, 765, 838, 866, 943, 996, 1016, 1017, 1039, 1044, 1101, 1184, 1188, 1224, 1335, 1352, 1420, 1486, 152 1, 1625, 1642, 1783, 2875, 3158, 3168, 3180, 3190, 3197
5	3.73, 1.09, 0.91	26, 102, 155, 262, 295, 332, 417, 462, 496, 611, 633, 714, 751, 821, 863, 871, 947, 969, 990, 994, 1017, 1044, 1133, 1175, 1214, 1249, 1302, 1326, 1373, 1381, 1449, 1464, 1476, 1577, 1631, 3047, 3102, 3152, 3162, 3175, 3188, 3734
6	6.08, 2.60, 1.82	227, 381, 389, 414, 524, 527, 629, 670, 741, 828, 829, 925, 970, 983, 1037, 1107, 1169, 1182, 1263, 1320, 1351, 1472, 1479, 1585, 1640, 3163, 3170, 3180, 3191, 3821
7	4.63, 2.16, 1.49	222, 268, 395, 441, 549, 550, 663, 722, 757, 811, 860, 891, 912, 930, 977, 1009, 1015, 1101, 1119, 1140, 1172, 1213, 1272, 1311, 1397, 1483, 1491, 1494, 1644, 1679, 3066, 3127, 3166, 3176, 3189, 3203
8	3.89, 1.31, 1.14	87, 94, 232, 365, 384, 401, 431, 580, 588, 684, 687, 774, 814, 839, 857, 886, 961, 970, 973, 983, 998, 1018, 1099, 1114, 1148, 1163, 1200, 1303, 1330, 1334, 1413, 1454, 1518, 1544, 1595, 3023, 3090, 3163, 3166, 3183, 3184, 3197
9	5.53, 2.79, 1.85	191, 380, 446, 484, 531, 598, 656, 802, 804, 805, 928, 984, 988, 1000, 1009, 1089, 1163, 1164, 1272, 1337, 1418, 1443, 1480, 1546, 1587, 3166, 3172, 3188, 3195, 3199
OH	560.5	3705
CH_2O	284.6, 39.0, 34.3	1202, 1270, 1539, 1827, 2870, 2919
TS1	4.38, 0.99, 0.85	i1767, 82, 96, 195, 241, 395, 412, 476, 583, 629, 653, 701, 756, 829, 850, 855, 904, 951, 987, 1008, 1013, 1045, 1081, 1116, 1166, 1183, 1193, 1233, 1321, 1351, 1375, 1484, 1520, 1612, 1631, 1957, 3066, 3160, 3170, 3180, 3192, 3204
TS2	3.82, 1.21, 0.94	i1274, 98, 178, 296, 351, 411, 432, 487, 498, 622, 676, 691, 749, 815, 859, 899, 927, 944, 990, 1018, 1039, 1044, 1106, 1159, 1178, 1205, 1257, 1286, 1323, 1361, 1461, 1466, 1475, 1585, 1628, 1639, 3020, 3102, 3156, 3166, 3181, 3189
TS3	3.59, 1.30, 0.98	i1229, 109, 162, 229, 311, 386, 417, 446, 490, 515, 613, 630, 706, 743, 822, 859, 935, 958, 969, 986, 1015, 1040, 1052, 1125, 1176, 1203, 1232, 1285, 1315, 1361, 1444, 1477, 1481, 1584, 1628, 2952, 3046, 3155, 3162, 3178, 3187, 3690,
TS4	4.57, 1.01, 0.83	i736, 78, 145, 160, 205, 222, 333, 391, 447, 490, 615, 628, 691, 734, 837, 8 55, 931, 963, 984, 985, 1020, 1035, 1081, 1121, 1160, 1173, 1215, 1263, 1314, 1353, 1454, 1480, 1504, 1598, 1645, 3042, 3087, 3161, 3169, 3186, 3193, 3796
TS5	3.81, 1.30, 1.14	i543, 124, 139, 202, 348, 387, 413, 438, 608, 637, 683, 731, 808, 815, 867, 899, 978, 987, 989, 992, 1021, 1031, 1112, 1164, 1165, 1195, 1210, 1324, 1336, 1365, 1450, 1476, 1512, 1555, 1595, 3005, 3074, 3168, 3174, 3185, 3191, 3197
TS6	3.78, 1.29, 1.13	i824, 127, 142, 186, 342, 390, 424, 437, 520, 613, 655, 661, 690, 744, 802, 819, 892, 973, 978, 989, 1018, 1027, 1083, 1094, 1122, 1171, 1172, 1189, 1302, 1338, 1462, 1477, 1492, 1563, 1597, 3047, 3161, 3166, 3172, 3187, 3192, 3197

TABLE 2: Zero-Point Corrected Relative Energies (kcal/mol) for the Intermediates and Transition States for the Reaction of Benzyl + O_2 System Calculated at Different Levels of Theories Optimized at B3LYP/6-311G(2d,d,p)

species	B3LYP/ 6-311G(2d,d,p)	CCSD(T)/ 6-31G+(d)	MP4SDQ/ 6-31G(d(f),p)	CBS-QB3
1 + O_2	0.0	0.0	0.0	0.0
2	−15.4	−19.4	−21.9	−22.3
3 + O	41.6	29.3	22	39.0
TS1	23.2	26.2	34.8	16.4
4 + OH	−43.1	−48.3	−60.1	−51.4
TS2	16.2	21.5	23.8	10.1
5	14.9	15.4	15.5	6.8
TS3	37.2	39.1	57.5	30.7
6 + OH	−31.3	−30.7	−33.3	−36.7
TS4	34.7	37.9	51.4	27.6
7 + OH	−7.1	−12.2	−23.4	−18.8
TS5	21.5	17.0	24.0	8.3
8	18.9	11.6	12.8	3.9
TS6	27.8	25.4	37.1	16.5
9 + CH_2O	−59.4	−63.2	−62.0	−65.4

Table 2 are also given in parentheses in Figure 1. Finally, the calculated results at the level of CBS-QB3 theory were summarized as the energy diagram for the benzyl + O_2 reactions in Figure 3. As shown in Figure 3, the relative roles of these dissociation pathways for the decomposition of benzylperoxy radicals could be qualitatively obtained. The heat of enthalpy for the reaction

$$C_6H_5CH_2 + O_2 \leftrightarrow C_6H_5CH_2OO \quad (6)$$

has already been experimentally determined to be −21.8 kcal/mol by Fenter et al.[14] and −20 kcal/mol by Elmaimouni et al.[16] The present relative energy for the reaction $C_6H_5CH_2 + O_2 \leftrightarrow C_6H_5CH_2OO$ obtained by the CBS-QB3 level of theory was −22.3 kcal/mol and was found to be in good agreement with the experimental results obtained by Fenter et al. and Elmanimouni et al. This agreement suggests that the relative energies obtained in the present work are accurate enough for the description of the potential energy surfaces for the benzyl + O_2 reaction. The heat of reaction for the direct O−O bond fission reaction from the $C_6H_5CH_2OO$ radical to form O atom and $C_6H_5CH_2O$ radical was 39.0 kcal/mol above the reactants; therefore, it is concluded that this reaction pathway was energetically unfavorable. On the other hand, the activation barriers for the other three plausible intramolecular isomerization reactions of the $C_6H_5CH_2OO$ radicals were found to be much lower than the direct O−O bond fission reaction $C_6H_5CH_2OO \rightarrow C_6H_5CH_2O + O$. Hence, it is expected that these three intramolecular isomerization reactions competed with each other when the temperature became high enough for the dissociation of the benzylperoxy radical (**2**).

According to the ROMP2//3-21G calculations by Clothier et al.[4] the activation barriers for the four-centerd isomerization reaction (channel B) was 6.9 kcal/mol relative to the reactants $C_6H_5CH_2 + O_2$. In the present study, the activation barrier height for reaction channel B at the CBS-QB3 level gives 16.4 kcal/mol above the reactants $C_6H_5CH_2 + O_2$, which is higher than those predicted by Clothier et al.[4] Since the CBS-QB3 level of theory is known as the high accuracy level of theory with an error of approximately ±1 kcal mol^{-1} for the G3 test set,[19,20] our predicted activation barrier height was expected to be more accurate than their estimates using the semiempirical quantum chemical calculations. The optimized structures for the C_6H_5-

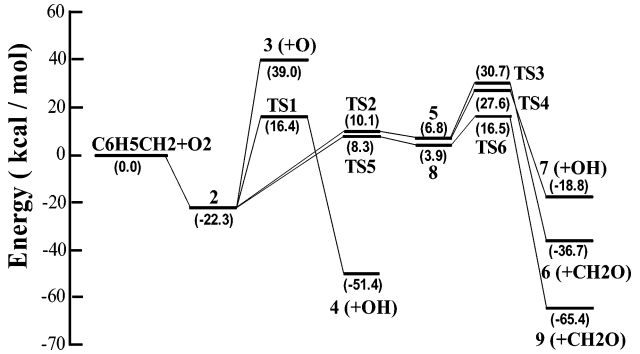

Figure 3. The potential energy surfaces for the reaction of benzyl with molecular oxygen calculated at the CBS-QB3 level of theory. The numbers in parentheses are the relative heat of formation relative to the reactants benzyl + O_2 and the units are in kcal/mol.

CHO−OH radicals formed after the four-centered isomerization reaction were also searched, but no stable structures were found in the present work. Therefore, it was concluded that benzaldehyde C_6H_5CHO (**4**) and OH radical were formed immediately after the four-centered isomerization reaction before stabilizing to the C_6H_5CHOOH radical.

The transition state for reaction channel C through the six-centered transition state, which abstracts the H atoms at the benzene ring, was also investigated at the same level of theory, and it was found that the barrier height of the transition state (**TS2**) relative to the reactants was 10.1 kcal/mol. Therefore, not only reaction channel B but also reaction channel C is important in the high-temperature oxidation of benzyl radicals. The subsequent reactions of the product **5** after the isomerization reaction through the **TS2** was also investigated, as depicted in Figures 1 and 3. Since the heat of reaction for the simple bond fission of the O−O bond from the $C_6H_4CH_2OOH$ radical is 51.0 kcal/mol endothermic relative to the reactants at the present CBS-QB3 level of theory, this reaction pathway is unimportant, even at higher temperatures. On the other hand, the barrier height for the transition state for the reaction forming HOC_6H_4 radical (**6**) and CH_2O molecules from the $C_6H_4CH_2OOH$ radical (**5**) was 30.7 kcal/mol above the reactants; thus, the decomposition forming product **6** and CH_2O radical might be important at higher temperatures. The other dissociation channels of the $C_6H_4CH_2OOH$ radical (**5**) were searched, and it was found that the barrier height of the transition state for reaction pathway forming cyclic-$C_6H_4(COH_2)$ molecule (**7**) and OH radical relative to the reactants was 27.6 kcal/mol and might play the key role in the high-temperature dissociation of the $C_6H_4CH_2$-OOH radical (**5**) as in the case of the reaction pathway forming HOC_6H_4 radical (**6**) and CH_2O molecule.

Reaction channel D, which forms the O_2 adduct (**8**) from the benzylperoxyl radical (**2**), has not been known so far. On the other hand, the important roles of the cyclization of the peroxy radicals to form the three-centered ring dioxiranyl radicals in the low-temperature oxidation of the aromatic as well as the unsaturated hydrocarbons were suggested by the recent theoretical investigation of several authors. Carpenter has carried out semiempirical quantum chemical calculations of the potential energy surface of the $C_2H_3 + O_2$[24] and phenyl (C_6H_5) + O_2[25] reaction for the first time and suggested the existence of a new reaction mechanism forming the three-centered ring dioxiranyl radical. The important roles of these new reaction pathways through the three-centered ring to form the dioxiranyl radicals were further confirmed by a higher level of G2M theory.[26,27] In the present work, we have also confirmed that the lowest activation barrier height among the three isomerization reactions

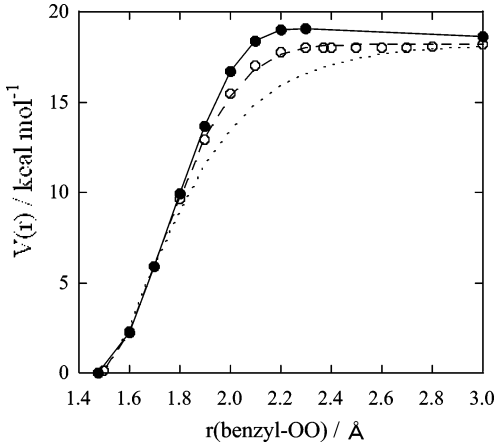

Figure 4. The benzyl−OO dissociation potential energy profile calculated using the B3LYP density functional with the 6-311G (d, p) basis set. The energy profile with C_s symmetry (●), the energy profile with C_1 symmetry (○), the Morse curve (dotted line), and the modified Morse function (dashed line).

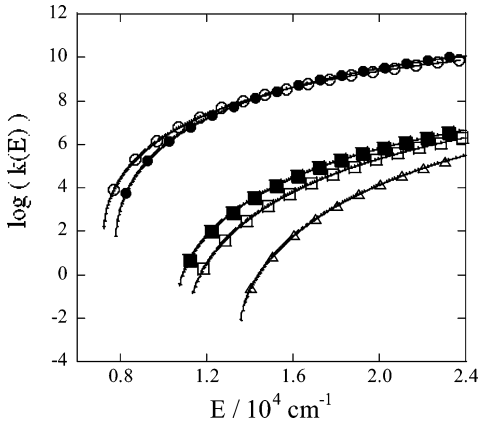

Figure 5. The microcanonical rate constants $k(E)$ for the backward and isomerization reactions for the benzylperoxy radicals as a function of the internal energy above benzylperoxy radicals: reaction channel B (Δ), reaction channel C (□), reaction channel D (■), backward reaction channel E at 300 K (●), and backward reaction channel E at 1500 K (○).

of the benzyl peroxyl radicals was the reaction pathway forming O_2-adduct (**8**), as shown in Figure 3, which was consistent with the previous theoretical results that the reaction channel that formed the dioxiranyl radicals played an important role in the aromatic and also the unsaturated hydrocarbons for the low-temperature oxidation reactions.

3.2. Mutichannel RRKM Calculations for the Isomerization Reaction of Benzylperoxy Radical. In the previous section, we discussed the possible roles of the isomerization and the subsequent dissociation reaction pathways of the benzylperoxy radical (**2**). However, in the low-temperature regimes, the backward reaction of the benzylperoxy radicals (channel E)

$$C_6H_5CH_2OO \rightarrow C_6H_5CH_2 + O_2 \qquad (-6)$$

also plays a key role in the decomposition reactions of the benzylperoxy radical (**2**).[9] Therefore, to discuss the relative roles of each decomposition channel of the benzylperoxy radical, we have to include the backward reaction (channel E). Figure 4 is the potential energy profiles for the dissociation reaction pathway E, $C_6H_5CH_2OO \rightarrow C_6H_5CH_2 + O_2$, without the zero-point energy correlations. For calculating the potential energy profiles in Figure 4, the length of the forming C−O bond was

TABLE 3: Benzyl−OO Distances, the Relative Energies Relative to the Total Energy of Benzylperoxy Radicals, the Rotational Constants, and the Vibrational Frequencies of the Variable Transition State of the Backward Reaction (E) of $C_6H_5CH_2OO \rightarrow C_6H_5CH_2 + O_2$

T/K	300	500	700	1000	1200	1500
r(R−OO)/Å	2.26	2.21	2.15	2.11	2.09	2.05
relative energy (kcal/mol)	22.23	22.08	21.77	21.36	21.12	20.63
rotational constant/GHz	2.89	2.92	2.95	2.98	2.99	3.00
	1.11	1.11	1.12	1.12	1.12	1.13
	1.01	1.01	1.01	1.02	1.02	1.02
	i186	i241	i301	i349	i366	i384
vibrational frequencies/cm^{-1}	43	44	47	49	50	51
	60	64	69	73	75	79
	101	106	111	116	119	123
	216	218	220	223	225	228
	318	333	344	349	350	351
	362	366	374	386	392	401
	408	409	410	411	411	412
	499	502	506	509	510	512
	543	546	550	555	558	563
	631	631	632	632	632	632
	648	672	695	696	697	698
	692	693	700	726	738	758
	765	768	770	772	772	774
	836	839	840	841	842	843
	839	840	842	844	844	846
	839	857	882	905	912	920
	918	920	924	932	938	956
	976	976	977	977	978	978
	977	979	982	985	987	990
	999	1000	1002	1003	1003	1004
	1007	1008	1010	1012	1012	1014
	1042	1043	1044	1044	1045	1045
	1118	1118	1118	1118	1118	1118
	1181	1181	1182	1183	1183	1183
	1194	1196	1197	1198	1199	1200
	1290	1288	1286	1284	1283	1280
	1339	1340	1341	1342	1342	1335
	1355	1355	1356	1356	1351	1342
	1431	1409	1383	1360	1357	1357
	1479	1479	1480	1481	1481	1481
	1493	1493	1493	1494	1494	1494
	1519	1520	1522	1524	1525	1526
	1594	1597	1600	1603	1604	1606
	1618	1622	1625	1629	1630	1632
	3157	3156	3155	3152	3151	3149
	3162	3163	3163	3163	3163	3163
	3168	3168	3169	3169	3169	3170
	3176	3177	3177	3178	3178	3178
	3183	3184	3185	3185	3185	3186
	3193	3193	3193	3194	3194	3194
	3255	3254	3251	3248	3247	3244

kept fixed at various values from 1.4 to 3.0 Å, while all other geometric parameters were optimized at the B3LYP/6-311G-(d,p) level of theory with C_s and C_1 symmetry. The energy was scaled so as that the absolute energy difference between benzyl + O_2 and benzylperoxy radical (**2**) was the same as the energy difference calculated by the CBS-QB3 level of theory. As shown in Figure 4, a very small barrier appeared in the dissociation potential energy profile for the $C_6H_5CH_2OO \rightarrow C_6H_5CH_2 + O_2$ reaction within the C_s symmetry, but when the symmetry was reduced to C_1 symmetry, the energy was monotonically and smoothly decreased as the O_2 molecule approached benzyl radicals until the benzylperoxy radicals were produced. Therefore, it was confirmed that the reaction rate for the backward reaction $C_6H_5CH_2OO \rightarrow C_6H_5CH_2 + O_2$ will be controlled by a variational transition state, the position of which will depend on the reaction temperature. To obtain a variational transition state at each temperature, analytical frequency calculations on the IRC for the reaction $C_6H_5CH_2OO \rightarrow C_6H_5CH_2 + O_2$ were performed at the B3LYP/6-311G(d, p) level of theory and the geometries that gave the maximum Gibbs free energy were searched. Table 3 summarizes the benzyl−OO distances, relative energies from the benzyl + O_2, rotational constants, and vibrational frequencies at the variable transition state for each temperature (i.e., 300, 500, 1000, 1200, and 1500 K), and these values were used for the RRKM/ME calculations for the backward reaction $C_6H_5CH_2OO \rightarrow C_6H_5CH_2 + O_2$.

Figure 5 is the dependence of the microcanonical rate constant $k(E)$ for backward reaction (−6) and also for the other three isomerization reaction pathways on the internal energy above benzylperoxy radical. As shown in Figure 5, the microcanonical rate constant for the backward reaction E was larger than the other isomerization reactions B−D for the whole temperature range. The temperature dependence of the microcanonical rate constant $k(E)$ for backward reaction (−6) was also calculated and it was found that the difference was very small compared to the difference of the microcanonical rate constant $k(E)$ between the backward and the other isomerization reactions. Among the isomerization reactions of the benzylperoxy radicals, the rate constant for reaction channel D was the largest and that for reaction channel C was the second largest. Reaction

TABLE 4: Calculated Rate Constants (cm^3 mol^{-1} s^{-1}) for the Dissociation Reactions of $C_6H_5CH_2OO$ (Channels B−E) and for the Reaction of $C_6H_5CH_2 + O_2 \rightarrow C_6H_5CH_2OO$

reaction channels	300 K	500 K	700 K	1000 K	1200 K	1500 K
			$P = 0.1$ atm			
2 → **4** + OH (channel B)	0	1.03×10^{-6}	4.66×10^{-3}	1.70×10^{-1}	4.85×10^{-1}	5.96×10^{-1}
2 → **5** (channel C)	5.05×10^{-13}	9.93×10^{-4}	1.36×10^{0}	2.94×10^{1}	6.94×10^{1}	8.29×10^{1}
2 → **8** (channel D)	1.43×10^{-11}	8.92×10^{-3}	8.95×10^{0}	1.69×10^{2}	3.69×10^{2}	4.54×10^{2}
2 → **1** (channel E)	3.74×10^{-4}	2.43×10^{3}	5.80×10^{5}	7.24×10^{6}	1.32×10^{7}	2.23×10^{7}
1 + O_2 → **2**	1.53×10^{11}	2.84×10^{11}	9.48×10^{10}	6.65×10^{9}	1.38×10^{9}	2.23×10^{8}
			$P = 1$ atm			
2 → **4**+OH (channel B)	0	8.23×10^{-6}	1.40×10^{-1}	1.50×10^{1}	5.43×10^{1}	9.41×10^{1}
2 → **5** (channel C)	5.48×10^{-13}	2.38×10^{-3}	1.04×10^{1}	6.17×10^{2}	1.84×10^{3}	2.97×10^{3}
2 → **8** (channel D)	1.50×10^{-11}	1.72×10^{-2}	5.03×10^{1}	2.49×10^{3}	6.85×10^{3}	1.11×10^{4}
2 → **1** (channel E)	3.75×10^{-4}	2.85×10^{3}	1.32×10^{6}	3.30×10^{7}	7.10×10^{7}	1.35×10^{8}
1 + O_2 → **2**	1.53×10^{11}	3.33×10^{11}	2.16×10^{11}	3.03×10^{10}	7.44×10^{9}	1.35×10^{9}
			$P = 10$ atm			
2 → **4** + OH (channel B)	0	1.53×10^{-5}	8.30×10^{-1}	4.10×10^{2}	2.24×10^{3}	5.95×10^{3}
2 → **5** (channel C)	5.52×10^{-13}	2.99×10^{-3}	2.87×10^{1}	6.30×10^{3}	2.72×10^{4}	6.28×10^{4}
2 → **8** (channel D)	1.50×10^{-11}	2.02×10^{-2}	1.17×10^{2}	1.95×10^{4}	7.60×10^{4}	1.71×10^{5}
2 → **1** (channel E)	3.75×10^{-4}	2.94×10^{3}	1.96×10^{6}	1.13×10^{8}	3.06×10^{8}	6.98×10^{8}
1 + O_2 → **2**	1.53×10^{11}	3.43×10^{11}	3.20×10^{11}	1.04×10^{11}	3.21×10^{10}	6.98×10^{9}
			High-Pressure Limit			
2 → **4** + OH (channel B)	5.30×10^{-17}	2.06×10^{-5}	1.76×10^{0}	7.25×10^{3}	1.02×10^{5}	5.85×10^{5}
2 → **5** (channel C)	7.65×10^{-13}	3.36×10^{-3}	4.31×10^{1}	5.04×10^{4}	5.31×10^{5}	2.60×10^{6}
2 → **8** (channel D)	1.75×10^{-11}	2.16×10^{-2}	1.58×10^{2}	8.07×10^{4}	4.20×10^{5}	1.01×10^{6}
2 → **1** (channel E)	4.01×10^{-4}	3.08×10^{3}	2.17×10^{6}	2.86×10^{8}	1.06×10^{9}	2.64×10^{9}
1 + O_2 → **2**	1.64×10^{11}	3.60×10^{11}	3.55×10^{11}	2.63×10^{11}	1.11×10^{11}	2.64×10^{10}

channel B, which was supposed to be the main reaction pathway according to the recent theoretical calculation by Clothier et al.,[4] was smallest.

3.3. Rate Constant Evaluations Using Master Equation Analysis. Using the microcanonical rate constant shown in Figure 5, the master equation analysis was performed at various temperatures and pressures. As was indicated in the section on the calculation methods, the single exponential down model was used as the collisional energy transfer model between the vibrationally excited benzylperoxy radical and the collision-partner N_2, which is the case in the normal combustion in air and the internal engines, and an average energy transferred per collision $\langle \Delta E_{down} \rangle$ in the single exponential down model was set to 500 cm^{-1} in our calculations.

The results of the rate constants for the backward dissociation reaction of the benzylperoxy radical (channel E) as well as the other dissociation channels B−D at various temperature and pressures were tabulated in Table 4. As shown in Table 4, the rate constant for reaction channel D was more than 2 orders of magnitude faster than the other isomerization channels B and C at 300 K, but the rate constant for reaction channel C became comparable to that for reaction channel D above 1000 K. The rate constant for the reaction of $C_6H_5CH_2 + O_2 \rightarrow C_6H_5CH_2$-OO was also computed from the equilibrium constants between $C_6H_5CH_2 + O_2$ and $C_6H_5CH_2OO$ estimated from the geometrical parameters at the B3LYP/6-311G(2d,d,p) level of theory and from the rate constants for the backward reaction for channel E. The calculated rate constant for the reaction of $C_6H_5CH_2 + O_2 \rightarrow C_6H_5CH_2OO$ was also tabulated in Table 4. Figure 6 is the summary of the plots of the rate constants for the reaction of $C_6H_5CH_2 + O_2 \rightarrow C_6H_5CH_2OO$ calculated in the present work. For comparison, the experimental results were also plotted in the same figure. The calculated rate constants for the reaction of $C_6H_5CH_2 + O_2 \rightarrow C_6H_5CH_2OO$ were reached at the high-pressure limits at the temperature range below 500 K, even at 0.1 atm, but above 500 K, the rate constants calculated at pressures between 0.1 and 10 atm deviated from the high-pressure limit and thus showed a negative temperature dependence. As shown in Figure 6, the agreement of the present work and the previous experiments was not good enough. The reason for such discrepancies is not clear, but the effect of chemical activations[28] was excluded, because the rate constant below 500 K, where the differences of the rate constants between the experiments and the present calculations were apparent, was already on the high-pressure limit and also all of the activation barriers of the benzylperoxy radical (**2**) were above the total energy of benzyl radical and O_2 molecule. It is well-recognized that not only the errors in the calculated energies but also the hindered rotations of the benzyl-OO bond angle have profound effects on the overall rate constant,[29,30] and the hindered rotor treatments on the rate evaluations will improve the errors. Further investigations should be done to clarify the reasons for such discrepancies.

The product branching ratios for CH_2O molecules and OH radicals formed by the high-temperature oxidation of benzyl radicals are very important for understanding the combustion of toluene. Therefore, attempts to evaluate the branching ratios for each reaction channel that forms CH_2O molecules or OH radicals were performed. To calculate the branching ratios for each reaction channel, the rate constants for the subsequent

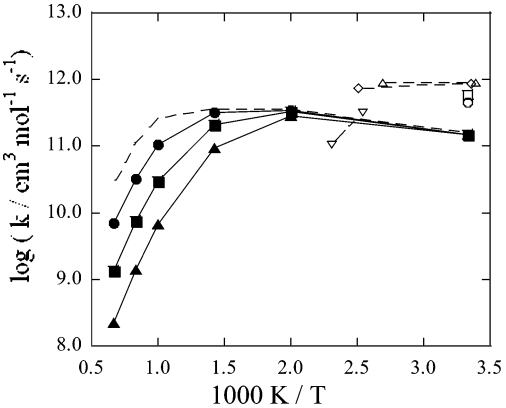

Figure 6. Arrhenius plot of the calculated rate constant for the benzyl + O_2 reaction: ●, $P = 7600$ Torr; ■, $P = 760$ Torr; ▲, $P = 76$ Torr; □, ref 12; Δ, ref 13; ◇, ref 14; ○, ref 15; and ▽, ref 16. The dashed line in the figure is the rate constant at the high-pressure limit.

TABLE 5: Calculated Rate Constants (cm^3 mol^{-1} s^{-1}) for the Dissociation Reactions of 5 and 8 (Channels F−J)

reaction channels	300 K	500 K	700 K	1000 K	1200 K	1500 K
			$P = 0.1$ atm			
5 → **6** + CH_2O (channel F)	0	1.03×10^{-7}	7.79×10^{-5}	5.86×10^{-3}	4.02×10^{-2}	2.81×10^{-1}
5 → **7** + OH (channel G)	0	8.60×10^{-5}	2.90×10^{-2}	1.98×10^{0}	1.23×10^{1}	7.69×10^{1}
5 → **2** (channel H)	2.87×10^{8}	7.67×10^{8}	1.21×10^{9}	1.57×10^{9}	2.05×10^{9}	3.12×10^{9}
8 → **9** + CH_2O (channel I)	4.68×10^{-2}	6.04×10^{1}	1.46×10^{3}	3.59×10^{4}	0	0
8 → **2** (channel J)	1.35×10^{8}	5.66×10^{8}	8.51×10^{8}	1.89×10^{9}	0	0
			$P = 1$ atm			
5 → **6** + CH_2O (channel F)	0	2.69×10^{-5}	6.01×10^{-3}	3.24×10^{-1}	1.60×10^{0}	1.23×10^{1}
5 → **7** + OH (channel G)	9.49×10^{-8}	1.53×10^{-2}	1.74×10^{0}	6.27×10^{1}	2.58×10^{2}	1.76×10^{3}
5 → **2** (channel H)	1.03×10^{9}	4.38×10^{9}	7.30×10^{9}	1.17×10^{10}	1.38×10^{10}	1.78×10^{10}
8 → **9** + CH_2O (channel I)	2.60×10^{0}	1.62×10^{3}	2.41×10^{4}	2.07×10^{5}	5.54×10^{5}	1.35×10^{6}
8 → **2** (channel J)	6.65×10^{8}	4.06×10^{9}	7.09×10^{9}	9.77×10^{9}	1.36×10^{10}	2.31×10^{10}
			$P = 10$ atm			
5 → **6** + CH_2O (channel F)	1.15×10^{-7}	1.13×10^{-1}	1.89×10^{1}	5.53×10^{2}	1.76×10^{3}	4.98×10^{3}
5 → **7** + OH (channel G)	1.38×10^{-4}	2.70×10^{1}	2.61×10^{3}	5.31×10^{4}	1.49×10^{5}	3.73×10^{5}
5 → **2** (channel H)	1.71×10^{9}	1.07×10^{10}	2.05×10^{10}	3.10×10^{10}	3.56×10^{10}	4.01×10^{10}
8 → **9** + CH_2O (channel I)	2.15×10^{2}	1.31×10^{5}	1.31×10^{6}	6.25×10^{6}	1.10×10^{7}	1.99×10^{7}
8 → **2** (channel J)	1.66×10^{9}	1.73×10^{10}	3.65×10^{10}	5.71×10^{10}	6.54×10^{10}	7.72×10^{10}
			High-Pressure Limit			
5 → **6** + CH_2O (channel F)	3.15×10^{-6}	3.26×10^{1}	3.49×10^{4}	5.81×10^{6}	4.54×10^{7}	3.60×10^{8}
5 → **7** + OH (channel G)	1.91×10^{-3}	3.59×10^{3}	1.91×10^{6}	1.96×10^{8}	1.22×10^{9}	7.92×10^{9}
5 → **2** (channel H)	2.32×10^{9}	1.90×10^{10}	4.76×10^{10}	8.48×10^{10}	1.15×10^{11}	1.60×10^{11}
8 → **9** + CH_2O (channel I)	2.74×10^{3}	2.12×10^{7}	1.07×10^{9}	2.13×10^{10}	6.90×10^{10}	2.25×10^{11}
8 → **2** (channel J)	2.37×10^{9}	6.13×10^{10}	2.49×10^{11}	7.12×10^{11}	1.07×10^{12}	1.60×10^{12}

reactions for reaction channels F−J in Figure 1 were calculated at various temperatures and pressures using the UNIMOL code as mentioned in the Calculation Methods.[21] The results were tabulated in Table 5. In order to estimate the product branching ratios for CH_2O molecules and OH radicals, the high-pressure limit rate constants for each reaction path tabulated in both Tables 4 and 5 were used. The product branching ratios for each channel were estimated from the stationary state approximation on the intermediate species of $C_6H_4CH_2OOH$ radical (**5**) and O_2-adduct (**8**). When the stationary state conditions are applied to the intermediate species of $C_6H_4CH_2$-OOH radical (**5**) and O_2-adduct (**8**), both d[**5**]/dt and d[**8**]/dt should be zero. Solving these equations, the product branching ratios forming the products **4**, **6**, **7**, and **9** can also be estimated. The results are shown in Figure 7. Although the rate constant for reaction channel B was smallest among all of the isomerization reaction channels B−E, the product branching yield forming benzaldehyde (**4**) and OH radical was around 0.7. The other important channels were the reaction channel that forms phenoxy radical (**9**) and CH_2O molecule. However, this branching ratio was around 0.3, which is half of the product yield of benzaldehyde (**4**) and OH radical. Also, the product branching ratio for the reaction channels forming HOC_6H_4 radical (**6**) and cyclic-$C_6H_4(COH_2)$ molecule (**7**) were calculated, and it was found that these reaction channels were of negligible importance, although the product branching ration forming cyclic-C_6H_4-(COH_2) molecule (**7**) and OH radical increases with temperature up to 12% at 1500 K.

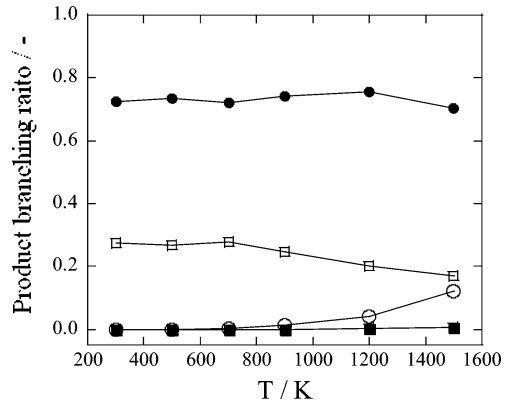

Figure 7. Temperature dependence of the calculated product branching ratios forming (a) benzaldehyde (**4**) and OH radical (●), (b) HOC_6H_4 radical (**6**) and CH_2O molecule (■), (c) cyclic-$C_6H_4(COH_2)$ molecule (**7**) and OH radical (○), and (d) phenoxy radical (**9**) and CH_2O molecule (□).

The important role of benzyl radicals in stimulating spontaneous ignition both of diesel and petrol engines was suggested by Pritchard's group.[31,32] They suggested the direct formation of OH from the following reactions

$$C_6H_5CH_2 + HO_2 \rightarrow C_6H_5CH_2O + OH \quad (2a)$$

$$C_6H_5CH_2 + O_2 \rightarrow C_6H_5CHO + OH \quad (3)$$

Our present calculations support their conclusions that reaction 3, which was described as reaction channel B in Figure 1, was one of the major channels forming OH radicals. It is now believed that the benzaldehyde (C_6H_5CHO, **4**) was mainly formed by the following reactions

$$C_6H_5CH_2 + HO_2 \rightarrow C_6H_5CH_2O + OH \quad (2a)$$

$$H + C_6H_5CH_2O \rightarrow C_6H_5CHO + H_2 \quad (7)$$

but our present calculations suggested that reaction 3 could also play some role in the benzaldehyde (C_6H_5CHO, **4**) formation. The present calculations also suggested the important role of the reaction channel forming phenoxy (C_6H_5O, **9**) and CH_2O molecules, whose reaction channel was not known so far. The CH_2O molecules increases the induction period to the cool flame,[33,34] while the formation of OH radicals enhances the ignition of the fuels.[35] Although the additional oxidation reactions of the intermediates **5** and **8**

$$C_6H_4CH_2OOH\ (\mathbf{5}) + O_2 \rightarrow C_6H_4(OO)CH_2OOH \quad (8)$$

$$O_2\text{-adduct}\ (\mathbf{8}) + O_2 \rightarrow C_6H_4OO(CH_2O_2) \quad (9)$$

were not included in the stationary state analysis of the product branching ratios to make the analysis simple, we hope that the

present calculations will give the chance to establish new combustion models for the ignition of the fuels containing toluene compounds.

4. Concluding Remarks

The high-temperature kinetics for the benzyl + O_2 reactions has been investigated at the CBS-QB3 level of theory. The potential energy diagram for the benzyl + O_2 reactions including the subsequent reactions of the decomposition of the benzylperoxy radicals were depicted. The computed heat of reactions for $C_6H_5CH_2 + O_2 \rightarrow C_6H_5CH_2OO$ was in good agreement with the previously determined experimental results within the errors of 1 kcal/mol. The rate constants for the dissociation reactions of the benzylperoxy radicals as well as the backward reaction (E) $C_6H_5CH_2OO \rightarrow C_6H_5CH_2 + O_2$ was calculated. The rate constant for the benzyl + O_2 reaction was also estimated from the predicted rate constant with the thermochemistry of the benzyl peroxide and then compared with the previous values obtained by experiments. Although the rate constant for reaction channel B was smallest, among the other isomerization reaction channels C−E, it was found that the product branching ratio for reaction channel B was 0.7, suggesting that reaction channel B could be one of the plausible pathways forming benzaldehyde from the benzyl + O_2 reaction, as suggested by Clothier et al.

Acknowledgment. One of the authors gratefully acknowledges the financial support by Sasaki Environmental Technology Foundations. This work was also supported in part by the 21st Century COE Program "Ecological Engineering for Homeostatic Human Activities" at Toyohashi University of Technology from the Ministry of Education, Culture, Sports, Science and Technology. A fruitful discussion with Prof. Mitsuo Koshi, The University of Tokyo, and Prof. William Pitz, Lawrence Livermore National Laboratory, is much appreciated.

References and Notes

(1) Brezinski, K. *Prog. Energy Combust. Sci.* **1986**, *12*, 1−24.

(2) Brezinski, K.; Litzinger, A.; Glassman, I. *Int. J. Chem. Kinet.* **1984**, *16*, 1053−1074.

(3) Barnard, J. A.; Ibberson, V. A. *Combust. Flame* **1965**, *9*, 149−157.

(4) Clothier, P. Q. E.; Shen. D.; Pritchard, H. O. *Combust. Flame* **1995**, *101*, 383−386.

(5) Muller-Markgraf, W.; Troe, J. *Symp. (Int.) Combust. (Proc.), 21st* **1986**, 815−824

(6) Muller-Markgraf, W.; Troe, *J. J. Phys. Chem.* **1988**, *92*, 4899−4905.

(7) Jones, J.; Bacskay, G. B.; Mackie, J. C. *J. Phys. Chem. A* ***1997***, *101*, *7105*.

(8) Oehlschlaeger, M. A.; Davidson, D. F.; Hanson, R. K. *J. Phys. Chem. A* **2006**, *110*, 6649−6653.

(9) Taajes, C.A. *J. Phys. Chem. A* **2006**, *110*, 4299−4312.

(10) Knyazev, V. D.; Slage, I. R. *J. Phys. Chem. A* **1998**, *102*, 1770−1778.

(11) Benson, S. W. *J. Phys. Chem.* **1996**, *100*, 13544−13547.

(12) Ebata, T.; Obi, K.; Tanaka, I. *Chem. Phys. Lett.* **1981**, *77*, 480−483.

(13) Nelson, H. H.; McDonald. J. R. *J. Phys. Chem.* **1982**, *86*, 1242−1244.

(14) Fenter, F. F.; Noziere, B.; Caralp, F.; Lesclaus, R. *Int. J. Chem. Kinet.* **1994**, *26*, 171−189.

(15) Hoyermann, K.; Seeba, J. J. *Symp. (Int.) Combust. (Proc.), 25st*, **1994**, 851−858.

(16) Elmaimouni, L.; Minetti, R.; Sawersyn, J. P.; Devolder, P. *Int. J. Chem. Kinet.* **1993**, *25*, 399−413.

(17) Frisch, M. J.; Trucks, G. W.; Schlegel, H. B.; Scuseria, G. E.; Robb, M. A.; Cheeseman, J.R.; Montgomery, J.A., Jr.; Vreven, T.; Kudin, K. N.; Burant, J. C.; Millam, J. M.; Iyengar, S. S.; Tomasi, J. Barone, V.; Mennucci, B.; Cossi, M.; Scalmani, G.; Rega, N.; Petersson, G. A.; Nakatsuji, H.; Hada, M.; Ehara, M.; Toyota, K.; Fukuda, R.; Hasegawa, J.; Ishida, M.; Nakajima, T.; Honda, Y.; Kitao, O.; Nakai, H.; Klene, M.; Li, X.; Knox, J. E.; Hratchian, H. P.; Cross, J. B.; Adamo, C.; Jaramillo, J.; Gomperts, R.; Stratmann, R. E.; Yazyev, O. Austin, A. J.; Cammi, R.; Pomelli, C.; Ochterski, J. W.; Ayala, P. Y.; Morokuma, K.; Voth, G. A.; Salvador, P.; Dannenberg, J. J.; Zakrzewski, V. G.; Dapprich, S.; Daniels, A. D.; Strain, M. C.; Farkas, O.; Malick, D. K.; Rabuck, A. D.; Raghavachari, K.; Foresman, J. B.; Ortiz, J. V.; Cui, Q.; Baboul, A. G.; Clifford, S.; Cioslowski, J.; Stefanov, B. B.; Liu, G.; Liashenko, A.; Piskorz, P.; Komaromi, I.; Martin, R. L.; Fox, D. J.; Keith, T.; Al-Laham, M. A.; Peng, C. Y.; Nanayakkara, A.; Challacombe, M.; Gill, P. M. W.; Johnson, B.; Chen, W.; Wong, M. W.; Gonzalez, C. and Pople, J. A. *Gaussian 03*, revision C.02, Gaussian, Inc., Wallingford, CT, 2004.

(18) Montgomery, J. A.; Frisch, M. J.; Ochterski, J. W.; Petersson, G. A. *J. Chem. Phys.* **1999**, *110*, 2822−2827.

(19) Montgomery, J. A.; Frisch, M. J.; Ochterski, J. W.; Petersson, G. A. *J. Chem. Phys.* **2000**, *112*, 6532−6542.

(20) Curtiss, L. A.; Raghavachari, K.; Redfern, P. C.; Rassolv, V.; Pople, J. A. *J. Chem. Phys.* **1998**, *109*, 7764−7776.

(21) Gilbert, R. G.; Smith, S. C.; Jordan, M. J. T. *UNIMOL Program Suite*, 1993 (calculation of falloff curves for unimolecular and recombination reactions). Available from the authors at School of Chemistry, Sydney University, NSW 2006, Australia or by e-mail to gilbert@chem.usyd.edu.au.

(22) Gilbert, R. G.; Smith, S.C. *Theory of Unimolecular and Recombination Reactions;* Blackwell Scientific: Oxford, 1990; p 318.

(23) Poling, B. E.; Prausnitz, J. M.; O'Connell, J. P. *The Properties of Gases and Liquids*; McGraw-Hill, New York, 2000.

(24) Carpenter, B. K. *J. Am. Chem. Soc.* **1993**, *115*, 9806−9807.

(25) Carpenter, B. K. *J. Phys. Chem.* **1995**, *99*, 9801−9810.

(26) Mebel, A. M.; Diau, E. W. G.; Lin., M. C.; Morokuma, K. *J. Am. Chem. Soc.* **1996**, *188*, 9759−9771.

(27) Tokamakov, I. V.; Kim, G. S.; Kislov, V. V.; Mebel, A. M.; Lin, M. C. *J. Phys. Chem. A* **2005**, *109*, 6114−6127.

(28) Matsumoto, K.; Klipperstein, S. J.; Tonokura, K.; Koshi, M. *J. Phys. Chem. A* **2005**, *109*, 4911.

(29) Fang, D. C.; Fu, X. Y. *J. Phys. Chem. A* **2002**, *106*, 2988.

(30) Maarten K.; Sabbe, A. G.; Vandeputte, R.; Veronique V. S.; Michel W.; Guy B. M. *J. Phys. Chem. A* **2007**, *111*, 8416.

(31) Davis, W. M.; Heck, S. M.; Pritchard, H. O. *J. Chem. Soc. Faraday Trans.* **1998**, *94*, 2725.

(32) Pritchard, H. O. *Phys. Chem. Chem. Phys*. **2006**, *8*, 4559.

(33) Griffiths, J. F.; Skirrow, G.; Tipper, C. F. H. *Combust. Flame* **1969**, *13*, 195.

(34) Kuwahara, K.; Ando, H.; Furutani, M.; Ohta, Y. *JSME Int. J. Ser. B* **2005**, *48*, 708.

(35) Wolfrum, J.; Volpp, H.R.; Rannacher, R.; Warnuts, J. *Gas Phase Chemical Reaction Systems*; Springer-Verlag: Berlin, 1996; p 279.